

1
3
5
7
9
11
13
15
17
19
21
23
25
27
29
31
33
35
37
39
41

Section V:
Environmental Biogeochemistry—
Concepts and Case Studies

1
3
5
7
9
11
13
15
17
19
21
23
25
27
29
31
33
35
37
39
41

Chapter 20

Understanding spatial variability and its application to biogeochemistry analysis

Sabine Grunwald, Rosanna L. Rivero and K. Ramesh Reddy

Abstract

Transforming the conceptual ideas of biogeochemical cycling into spatially explicit context has been hampered by ecosystem complexity, multiple nested levels of interrelated physical, biological and chemical processes, and the lack of sufficient quantitative data. The mosaic of ecosystem structures and functions distributed across a landscape represent the combined effects and interactions of a variety of biotic and abiotic factors. As a result, existing landscape patterns implicitly contain information about the processes that generated these patterns. Deductive science has generated extensive knowledge of how individual parts of aquatic ecosystem's function derived from site-specific studies. Yet, understanding of how the parts interact as a whole requires a holistic perspective that considers the spatial variability, distribution and interaction of all components of a landscape. The predicament entailed by the complexity of aquatic ecosystems requires a synergistic approach that integrates knowledge from different disciplines including biogeochemistry, geography, statistics/geostatistics, ecology, hydrology and others. Interdisciplinary collaboration will be key to reconcile deductive and inductive science and allow us to understand the linkages between biogeochemical properties and processes at landscape scale. In this chapter we provide an overview of a variety of geostatistical and hybrid methods that can be used to characterize the spatial variability, distribution and uncertainty of biogeochemical properties. A case study demonstrates the application of these methods to predict soil total phosphorus across a wetland in the Greater Everglades.

1 **20.1. Introduction**

3 Conceptually, scale represents the *window of perception*, the filter, or the
5 measuring tool through which a landscape may be viewed or perceived
7 (Levin, 1992). Thus, changing the scale changes the properties that we
9 observe—the patterns of reality, which has implications for understand-
11 ing the dynamics of any environmental system. Since parameters and
13 processes important at one scale are frequently not important or predic-
15 tive at another, it is essential to gain a better understanding of the spatial
17 variability and distribution of ecosystem properties. Turner et al. (1989)
19 pointed out that ecological problems often require the upscaling of fine-
21 scale measurements for the analysis of coarse-scale phenomena. A holistic
23 view of landscapes is required to understand ecosystem processes at mi-
25 cro, meso and macro spatial scales.

15 Biogeochemistry is defined as the scientific study of the interactions
17 among the biological, geological and chemical systems of Earth, including
19 the cycling of matter and energy through them. Numerous conceptual
21 models have been developed that describe the cycling of matter and ma-
23 terial in aquatic ecosystems (Mitsch and Gosselink, 2000). The carbon
25 (C), nitrogen (N), phosphorus (P) cycles play a critical role in the func-
27 tioning of wetland ecosystems, their structure, resilience and sensitivity to
29 natural and human-induced disturbances.

23 In this chapter we discuss the importance of spatially explicit mapping
25 of biogeochemical properties that applies to aquatic and terrestrial ec-
27 osystems in the context of spatial autocorrelation and covariation of these
29 properties. Understanding the spatial variability and distribution of
31 biogeochemical properties is a necessity for holistic assessment of envi-
33 ronmental quality at landscape-scale.

31 **20.2. Concepts and methods**

33 The mosaic of system structures and functions distributed across a land-
35 scape represent the combined effects and interactions of a variety of biotic
37 and abiotic factors. As a result, existing landscape patterns implicitly
39 contain information about the processes that generated these patterns
41 (Holling and Gunderson, 2002). Spatial and temporal ecosystem at-
tributes are neither uniform nor scale independent. Likewise, biogeo-
chemical properties and processes vary gradually and continuously in
space and time. Discrete boundaries that cause abrupt shifts from high to
low values of physico-chemical and biological properties are limited to
crisp physical boundaries (e.g., hydrologic boundaries, land use) or

1 anthropogenic disturbances. To restrict observations to few sites (e.g.,
2 along a transect) limits the ability to capture the biogeochemical signa-
3 tures of a landscape.

4 Some biogeochemical properties are labor-intensive and costly to de-
5 rive (e.g., phosphorus fractionation schemes, alkaline phosphatase activ-
6 ity) whereas other measurements are standard routine (e.g., bulk density,
7 total phosphorus—TP). Hence, in the past, numerous studies focused on
8 sparse spatially distributed sampling or experimental lab/field studies to
9 understand biogeochemical cycling (Reddy et al., 1998; White and Reddy,
10 2000; Fisher and Reddy, 2001; Craft and Chiang, 2002; Karathanasis et
11 al., 2003; Morris et al., 2004) resulting in a tremendous amount of
12 knowledge. The strength of such site-specific studies is to describe feed-
13 back processes in response to a localized change in biogeochemical con-
14 ditions. For example, changing plant communities provide feedback on
15 soil biogeochemical properties and microbial communities that respond
16 to changing environmental conditions (e.g., organic matter, hydroperiod,
17 temperature, light, etc.). Numerous site-specific studies have ignored the
18 *spatial* interrelationships, i.e., the *spatial covariation*, among different
19 biogeochemical properties and assume independence of observations.
20 Deductive science has generated extensive knowledge of how individual
21 parts of aquatic ecosystems function (compare Eq. (1)). Yet, understand-
22 ing of how the parts interact as a whole requires a holistic perspective that
23 considers the spatial interaction of all components of a landscape. Trans-
24 forming the conceptual ideas of biogeochemical properties and processes
25 into spatially explicit context has been hampered by ecosystem complex-
26 ity, multiple nested levels of interrelated physical, biological and chemical
27 processes, and the lack of sufficient quantitative data.

$$28 \quad y(x_i) = f\{z_j(x_i)\} \quad (1)$$

29 where $y(x_i)$ is the response variable observed at location x_i and $z_j(x_i)$ the
30 biogeochemical properties ($j = 1, 2, 3, \dots, n$) observed at location x_i .

31 **20.2.1. The concept of spatial autocorrelation**

32 The deductive approach is rooted in the concept developed by Fisher
33 (1925), who pointed out the importance of random selection ensuring that
34 estimates are unbiased. This assumption of independence is a prerequisite
35 for many statistical tests including regression analysis, analysis of var-
36 iance, t -tests and others (Berthouex and Brown, 2002). Classical statistical
37 methods have been used extensively to document significant differences in
38 biogeochemical properties/behavior using controlled experiments (e.g.,
39 mesocosms), plots, or blocks. Such analyses are based on the assumption
40
41

1 that the investigated properties show no spatial autocorrelation. *Spatial*
2 *autocorrelation* is a term referring to the degree of relationship that exists
3 between two or more spatial variables, such that when one changes, the
4 other(s) also change (Webster and Oliver, 2001). This change can either
5 be in the same direction, which is a positive autocorrelation, or in the
6 opposite direction, which is a negative autocorrelation (Burrough, 1986;
7 Isaaks and Srivastava, 1989). Popular measures of spatial autocorrelation
8 are Moran's I (Moran, 1950) and Geary's C (Geary, 1954) coefficients.
9 Positive values of Moran I and value smaller than 1 for Geary's C co-
10 efficient correspond to positive autocorrelation. True spatial independ-
11 ence of properties in aquatic and terrestrial landscapes does not really
12 exist due to the interconnectedness of biogeochemical processes of N, C
13 and P and other nutrients and transport processes that move water, ma-
14 terial and energy through the ecosystem. Rather, the sampling density
15 and spacing between observations determine if the underlying spatial
16 autocorrelation can be captured by a model or not. Studies that limit
17 observations to sparse sampling locations far apart from each other ig-
18 nore spatial autocorrelation and focus on the identification of significant
19 differences between sites with contrasting biogeochemical conditions.
20 However, numerous studies documented that spatial autocorrelation of
21 biogeochemical soil properties is inherent at landscape scale [$> 1 \text{ km}^2$]
22 (Newman et al., 1997; DeBusk et al., 2001; Grunwald et al., 2004, in
23 press; Bruland and Richardson, 2005). To identify spatial autocorrelation
24 of a specific biogeochemical property, observations need to be collected
25 with a spatially distributed design throughout an ecosystem that accounts
26 for short-, medium- and long-range variability. Constraining biogeo-
27 chemical observations to few point locations (sites) cannot possibly ex-
28 plain the underlying spatial autocorrelation of properties as well as
29 interrelationships between different biogeochemical properties (e.g., TP
30 and labile P), which is called the spatial covariation. The predicament
31 entailed by the complexity of aquatic and terrestrial ecosystems requires a
32 synergistic approach integrating knowledge from different disciplines in-
33 cluding biogeochemistry, geography, statistics/geostatistics, ecology, hy-
34 drology and others. Interdisciplinary collaboration will be key to
35 reconcile deductive and inductive science to understand the linkages be-
36 tween properties and processes at landscape scale. Each soil biogeo-
37 chemical property exhibits specific behavior of spatial autocorrelation
38 that is related to environmental factors such as nutrient cycling, hydro-
39 logy, topography, anthropogenic-induced nutrient inputs, vegetation
40 types, etc. and spatial scale. For example, TP showed long-range corre-
41 lation lengths across the Water Conservation Area-2A (WCA-2A), a
wetland in the northern Everglades, in 1990 and 1998 with spatial

1 autocorrelations of 6500 and 7549 m, respectively (Grunwald et al., 2004).
 2 Similar long-range spatial autocorrelation for TP was found in the Blue
 3 Cypress Marsh Conservation Area, a wetland in eastern Florida, with
 4 7240 m (Grunwald et al., in press).

5 20.2.2. The concept of regionalized variable theory

7 We can formalize the concept of spatial variation outlined above using
 8 the theory of regionalized variables (Webster and Oliver, 2001). Since the
 9 environment and its component attributes result from many interactive
 10 physical, chemical and biological processes that are non-linear and/or
 11 chaotic, the outcome is so complex that the variation appears to be ran-
 12 dom. If we adopt a stochastic view then at each point in geographic space
 13 there is not just one value for an attribute but a whole set of values.
 14 Consider a region R that comprises an infinite number of points x_i , $i = 1$,
 15 $2, \dots, \infty$. Whereas in the classical statistical approach the values of an
 16 observed biogeochemical attribute, z , at these points constitute the popu-
 17 lation, in the geostatistical approach this population is assumed to be
 18 just one realization of a random process or random function that could
 19 generate any number of such populations. Then, at each place x_0 the
 20 attribute is considered a random variable $Z(x_0)$. Thus, at a location x_0 a
 21 biogeochemical attribute is treated as a random variable with mean (μ), a
 22 variance (σ^2) and a cumulative distribution function (cdf). Note, that the
 23 actual value $z(x_0)$ is just one drawn at random from that distribution. The
 24 set of random variables, $Z(x_1), Z(x_2), \dots, Z(x_n)$ constitute a random func-
 25 tion or a stochastic process (Webster and Oliver, 2001). Regionalized
 26 variable theory assumes that the spatial variation of any biogeochemical
 27 variable can be expressed as the sum of three major components (Eq. (2))
 28 (Burrough and McDonnell, 1998): (i) a structural component having a
 29 constant mean or trend that is spatially dependent, (ii) a random, but
 30 spatially correlated component, known as the variation of the regional-
 31 ized variable and (iii) a spatially uncorrelated random noise or residual
 32 term. A non-stationary trend extends over the whole study area and is
 33 therefore called a global model. In contrast, local trends, also called drift,
 34 describe localized variation (Webster and Oliver, 2001). [Note: a header
 35 “ \hat{Z} ” indicates that the variable is estimated]

$$37 \quad \hat{Z}(x_i) = m(x_i) + \varepsilon'(x_i) + \varepsilon'' \quad (2)$$

39 where $\hat{Z}(x_i)$ is the value of a random variable at locations x_i with $i = 1$,
 40 $2, \dots, n$; $m(x_i)$ the trend model—deterministic function describing the
 41 “structural” component of $\hat{Z}(x_i)$; $\varepsilon'(x_i)$ the stochastic, locally varying but
 spatially dependent component (the regionalized variable); ε'' the A

1 residual, spatially independent noise term having zero mean and variance;
 2 and x_i the geographic position in 1, 2 or 3 dimensions.

3 Observations obtained close to each other are more likely to be similar
 4 than observations taken further apart from each other. This spatial cor-
 5 relation of $\varepsilon'(x_i)$ is described by the semivariance $\hat{\gamma}(h)$ (Eq. (3)). If γ is
 6 plotted as a function of the lag distance h that separates x_i and x_i+h , the
 7 semivariogram is obtained. One implicit assumption is that the mean,
 8 variance and covariance depend only on the separation distance h and not
 9 on the absolute position. This assumption constitutes second-order station-
 10 arity (Isaaks and Srivastava, 1989). $\hat{\gamma}(h)$ is estimated as

$$\hat{\gamma}(h) = \frac{1}{2N(h)} \sum_{i=1}^{N(h)} [z_u(x_i) - z_u(x_i + h)]^2 \quad (3)$$

15 where $\hat{\gamma}(h)$ is the semivariance at lag h ; h the distance between data pairs
 16 ($z_u(x_i) - z_u(x_i + h)$) (or lag); N the total number of data pairs ($z_u(x_i) -$
 17 $z_u(x_i + h)$); and $z_u(x_i)$ the biogeochemical variable u .

18 Commonly, least square fitting of the experimental semivariogram
 19 model is used. However, visual inspection of the statistical fitting process
 20 is essential. Alternatively, interactive fitting can be used to model the
 21 semivariogram. Characteristic parameters that can be derived from semi-
 22 variograms are the *nugget*, *sill* and *range*. The nugget describes the meas-
 23 urement error and fine-scale variability. Semivariograms of properties or
 24 processes that exhibit second-order stationarity reach upper bounds at
 25 which they remain after their initial increases. This upper bound, or
 26 maximum is known as the sill. The range describes the spatial autocor-
 27 relation and marks the limit of spatial dependence (Webster and Oliver,
 28 2001). The univariate semivariance can be extended to consider two
 29 biogeochemical variables, z_u and z_v , to derive the cross-semivariances
 30 $\hat{\gamma}_{uv}(h)$.

$$\hat{\gamma}_{uv}(h) = \frac{1}{2N(h)} \sum_{i=1}^{N(h)} [z_u(x_i) - z_u(x_i + h)][z_v(x_i) - z_v(x_i + h)] \quad (4)$$

35 Regionalized variable theory and semivariogram analyses are described
 36 in detail by Goovaerts (1997), Chilès and Delfiner (1999), Webster and
 37 Oliver (2001, 2005). The semivariogram provides input for kriging, which
 38 is a weighted interpolation technique to create continuous prediction
 39 maps of biogeochemical properties. Major limitations of the univariate
 40 geostatistical technique of kriging are due to the assumption of station-
 41 arity, which is often not met by the field-sampled datasets and the large
 amount of data (> 100 observations; recommended > 150 observations)

1 required to characterize the spatial autocorrelation of a property (Webster and Oliver, 2001).

3

20.2.3. *Global models*

5

7 Global models use all available observations to provide predictions for
9 the whole area of interest, while local interpolators operate within a small
11 zone around the point being interpolated to ensure that estimates are
13 made only with data from locations in the immediate neighborhood
15 (Burrough and McDonnell, 1998). Trend surfaces are the simplest global,
17 geospatial model that requires fitting some form of polynomial equation
19 through biogeochemical attribute values. These are least square methods
21 that model the long-range spatial variation. Such models assume that the
23 spatial coordinates are the independent variables and z (attribute of interest) is the dependent variable (Webster, 1994). As trend surfaces are simplified representations of reality, it is difficult to ascribe any physical meaning to complex, higher-order polynomials. Therefore, the main use of trend surface analysis is not as an interpolator, but as a way of removing broad features of the data prior to using some complex local interpolator. The concept is based on partitioning the variance between trend and the residuals from the trend. Compare Eq. (2) that partitions the variability of a property into (i) a global trend component, (ii) stochastic, locally varying but spatially dependent component and (iii) a residual noise term.

25

20.2.4. *Local models*

27

29 Local, deterministic interpolation methods focus on modeling short-range local variations. The interpolation involves: (i) defining a search neighborhood around the point to be interpolated, (ii) finding the observations within this neighborhood, (iii) choosing a mathematical function to represent the variation over this limited number of points or area, and (iv) evaluating it for the point on a regular grid. The procedure is repeated until all the points on a grid have been computed (Burrough and McDonnell, 1998). For example, commonly used local interpolation methods are inverse distance weighting (IDW), splines and kriging (Burrough and McDonnell, 1998). Splines (local fitting functions) estimate values using a mathematical function that minimizes overall surface curvature, resulting in a smooth surface that passes exactly through the observation points, while at the same time ensuring that the joins between one part of the curve (or surface) and another are continuous. In contrast to trend surfaces and weighted averages, splines retain small-scale

41

1 features. A disadvantage of splines and IDW is that there are no direct
 2 estimates of the errors associated with these forms of interpolation (Bur-
 3 rough and McDonnell, 1998). Local interpolators in its simplest form are
 4 based weights that are computed from a linear function of distance be-
 5 tween sets of data points and the point to be predicted (Eq. (5)).

$$7 \quad \hat{Z}(x_0) = \sum_{i=1}^n \lambda_i * z(x_i) \quad \sum_{i=1}^n \lambda_i = 1 \quad (5)$$

9 where $\hat{Z}(x_0)$ is the predicted attribute value at unsampled location x_0 ; λ_i
 10 the weights; $z(x_i)$ the observed attribute value at locations x_i ; and n the
 11 number of observations.

12 In Eq. (5) $z(x_1), z(x_2), \dots, z(x_n)$ are the measured values of the biogeo-
 13 chemical property z at locations x_1, x_2, \dots, x_n and λ_i are the weights that
 14 sum to 1 to assure unbiasedness. The expected error is $E[\hat{Z}(x_0) -$
 15 $Z(x_0)] = 0$ and the prediction variance is

$$17 \quad \text{var}[\hat{Z}(x_0)] = E\{[\hat{Z}(x_0) - Z(x_0)]^2\}$$

$$18 \quad = 2 \sum_{i=1}^N \lambda_i \gamma(x_i, x_0) - \sum_{i=1}^N \sum_{j=1}^N \lambda_i \lambda_j \gamma(x_i, x_j) \quad (6)$$

21 where $\gamma(x_i; x_0)$ is the semivariance of Z between the i th sampling point
 22 and the target point x_0 at an unsampled location and $\gamma(x_i; x_j)$ the semi-
 23 variance of Z between sampling points x_i and x_j .

25 **20.2.5. Kriging**

27 Kriging is a generic term adopted by geostatisticians for a family of
 28 generalized least-squares regression algorithms. In the kriging system the
 29 goal is to minimize the kriging variance, where the weights sum to 0 (Eq.
 30 (7)).

$$31 \quad \sum_{i=1}^n \lambda_i(x_i; x_j) - \psi(x_0) \quad \text{with} \quad \sum_{i=1}^n \lambda_i = 0 \quad (7)$$

35 where $\psi(x_0)$ is the Lagrange multiplier.

36 All kriging estimators are but variants of the basic linear regression
 37 estimator $\hat{Z}(x_0)$ defined as

$$38 \quad \hat{Z}(x_0) - m(x_0) = \sum_{i=1}^n \lambda_i(x_0)[Z(x_i) - m(x_i)] \quad (8)$$

41 where $\hat{Z}(x_0)$ is the linear regression estimator at unsampled location x_0
 and $\lambda_i(x_0)$ the weights assigned to datum x_0 interpreted as a realization of

1 the random variable $Z(x_i)$ and located within a given neighborhood $W(x)$ centered on x .

3 The weights are chosen to minimize the error variance $\sigma^2(x_0) = \text{var}\{\hat{Z}(x_0) - Z(x_0)\}$ under the constraint of unbiasedness of the estimator.
5 These weights are obtained by solving simultaneously a system of linear equations which is known as the kriging system (Goovaerts, 1999).

7 The local neighborhood characteristics including (i) the number of observations ($z(x_i)$) within a neighborhood, (ii) major and minor semiaxis (size of the neighborhood) and (iii) the neighborhood shape (uniform or discretized into subunits) determine the strengths of smoothing. In general, a small neighborhood generates localized predictions based on few observations, which are prone to the influence of extreme values producing blocky/crisp looking maps. In contrast, large neighborhoods smooth over a larger area providing conservative predictions for areas with high observed values.

17 20.2.6. Kriging variants

19 Differences in kriging variants reside in the model considered for the trend $m(x)$ (Goovaerts, 1999):

- 21 (a) *Simple kriging (SK)* considers the mean $m(x)$ known and constant throughout the study area.
23 (b) *Ordinary kriging (OK)* accounts for local fluctuations of the mean by limiting the domain of stationarity of the mean to the local neighborhood ($W(x)$). The mean is considered constant but unknown.
25 (c) *Universal kriging (UK)*, also known as kriging with a trend model, considers that the unknown local mean $m(x')$ smoothly varies within each local neighborhood, and the trend is modeled as a linear combination of functions $f_k(x)$ of the coordinates

$$31 \quad m(x') = \sum_{k=0}^K a_k(x') f_k(x') \quad (9)$$

35 with $a_k(x')$ constant within each local neighborhood $W(x)$ but unknown.

- 37 (d) *Regression kriging (RK)*: Alternatively, the trend function $m(x)$ can be modeled separately, where kriging is combined with regression or a regression variant (Odeh et al., 1994, 1995; Odeh and McBratney, 2000; Hengl et al., 2004). The deterministic component $m(x)$ is considered dependent on some exogenous factors such as climate, hydrology, topography, vegetation or other environmental factors that

1 can be described via multivariate regression, Generalized Linear
 3 Models, Classification and Regression Trees, Generalized Additive
 5 Models or other functions. Odeh et al. (1994, 1995) defines regression
 kriging where model $f(\cdot)$ is used to describe the relationship between
 predictors and environmental factors:

$$7 \quad \hat{Z}(x_i) = f(Q, x_i) + \hat{R}(x_i) \quad (10)$$

9 where $f(Q, x_i)$ is the function describing the structural component
 of $\hat{Z}(x_i)$ as a function of Q environmental variables at location x_i ;
 11 $\hat{R}(x_i)$ the stochastic, locally varying but spatially dependent residual
 from $f(Q, x_i)$. In RK, the target biogeochemical property at an un-
 13 visited site is first predicted by $f(\cdot)$, followed by kriging of the residuals
 of the model.

- 15 (e) *Kriging with an external drift (KED)* models the trend $m(x)$ as a linear
 function of a smoothly varying secondary (external) variable $y(x)$
 17 instead of a function of the spatial coordinates. Besides the difficult
 inference of the residual semivariogram, this method requires that the
 19 relation between the primary trend and secondary variable is linear
 and makes physical sense (Goovaerts, 1999). In KED the secondary
 21 exhaustive data are only used to inform on the shape of the trend of
 the primary variable. In contrast, cokriging exploits more fully the
 23 secondary information by directly incorporating the values of the
 secondary variable and measuring the degree of spatial association
 25 with the primary variable through the cross-semivariogram. Cokri-
 27 ging is the extension of ordinary kriging of a single variable to two or
 more variables. There must be some kind of coregionalization among
 the variables for it to be profitable. It is particularly useful if some
 29 property that is cheap to measure (e.g., remote sensing image) is spa-
 31 tially correlated with another property that is expensive to measure
 and/or labor intensive to collect and available at many fewer sites
 (Webster and Oliver, 2001).

QA :1

33
 35 In many environmental applications a few hot spots (high values) co-
 exist with many small values that vary continuously in space. Depending
 37 on whether large values are clustered or scattered in space, our physical
 interpretation of the biogeochemical processes controlling high and low
 39 values may change. The characterization of the spatial distribution of z -
 values above or below a given threshold value z_k requires prior coding of
 41 each observation as an indicator datum $ind(x_i; z_k)$ defined as (Goovaerts,
 1999):

$$\begin{aligned} \text{ind}(x_i; z_k) &= 1 && \text{if } z(x_i) \leq z_k \\ &= 0 && \text{otherwise} \end{aligned} \quad (11)$$

Indicator semivariograms can be computed by substituting indicator data $\text{ind}(x_i; z_k)$ for z -data:

$$\hat{\gamma}(h, z_k) = \frac{1}{2N(h)} \sum_{i=1}^{N(h)} [\text{ind}(x_i; z_k) - \text{ind}(x_i + h; z_k)]^2 \quad (12)$$

The indicator variogram value $\hat{\gamma}(h, z_k)$ measures how often two z -values separated by a vector h are on opposite sides of the threshold value z_k .

20.2.7. Spatial stochastic simulations

Least-square interpolation algorithms such as kriging tend to smooth out local details of the spatial variation of the attribute, with small values typically overestimated and large values underestimated (Isaaks and Srivastava, 1989). This is a serious shortcoming if large pollutant concentrations or biogeochemical property values are of interest. Kriging aims at local accuracy through minimizing a covariance-based error variance, while spatial stochastic simulation aims at reproducing spatial structure through a covariance model. Unlike kriging, spatial conditional stochastic simulations do not aim at minimizing a local error variance but focus on the reproduction of statistics such as the sample histogram or the semivariogram model in addition to honoring of data values. The output results, i.e., a set of alternative realizations, provide a visual and quantitative measure of the spatial uncertainty. A probability distribution (ccdf) for attributes at a particular location can be built for a set of multiple realizations of the joint distribution of attribute values in space (Goovaerts, 1997). Kriging produces one output map. In contrast, stochastic simulation generates multiple realizations of the spatial distribution of (biogeochemical) attribute values and it uses differences among simulated maps as a measure of uncertainty. Therefore, kriging is preferred for local estimation whereas simulation is increasingly preferred for assessment of spatial uncertainty and reproduction of global statistics, risk assessment, flow modeling and water quality simulation modeling (Goovaerts, 1997; Grunwald et al., 2004; Chilès and Allard, 2005). The latter situations require knowledge about the uncertainty of environmental attribute values at many locations simultaneously (multiple-point or spatial uncertainty).

Conditional Sequential Gaussian Simulation (CSGS) is a stochastic simulation method for the generation of partial realizations using normal

1 random functions. The method uses the Gaussian model type and is
2 ergodic, which means that simulations have a sample mean close to the
3 theoretical mean and a sample covariance to the theoretical covariance
4 $C(h)$. This implies that all simulations are drawn from the realizations of a
5 random function that is ergodic in the mean value and the covariance
6 (second-order ergodicity) (Chilès and Delfiner, 1999). Conditioning is the
7 operation that ensures that simulation values match values at sample
8 points. Conditional Sequential Gaussian Simulation provides a measure
9 of local uncertainty because each conditional cdf relates to a single spatial
10 location x .

11 **20.2.8. Summary**

12
13 A flow chart that provides an overview of statistical, geostatistical and
14 hybrid geospatial modeling techniques presented above is shown in
15 Fig. 20.1. Depending on the spatial autocorrelation and the spatial co-
16 variation, different methods are suggested to generate the best possible
17 predictions of biogeochemical properties within a given aquatic ecosys-
18 tem. Many variations of these methods exist that can be further explored
19 in Goovaerts (1997), Webster and Oliver (2001, 2005), McBratney et al.
20 (2000, 2003) and Grunwald (2005).

23 **20.3. Case study**

24
25 In this case study we illustrate the concepts and methods outlined above
26 to characterize spatial variability of TP within a subtropical wetland,
27 WCA-2A, located in the Greater Everglades, Florida. The Everglades is a
28 naturally P-limited aquatic ecosystem that has been impacted by nutrient
29 inputs from agricultural land use over the last decades (Noe et al., 2001).
30 In addition, this system has been manipulated hydrologically (canals,
31 levees, hydrologic control structures) altering the historic uninterrupted
32 sheet flow through the whole system (Porter and Porter, 2002). Water
33 Conservation Area-2A is 418 km² in size consisting primarily of Histosols
34 (soils with at least 12–18% organic C by weight), which developed during
35 the past 5000 years (McCollum et al., 1976). Vegetative communities are
36 dominated by sawgrass (*Cladium jamaicense* Crantz), cattail (*Typha* spp.),
37 mixed sawgrass and cattail communities and few tree islands (Porter and
38 Porter, 2002). The wetland is surrounded by canals and levees with two
39 major surface water inflow points (S-7 and S-10 pump stations). Water
40 moves through WCA-2A as sheet flow from the north-east to the outflow
41 located south (DeBusk, 2001). Elevated soil P concentration in WCA-2A

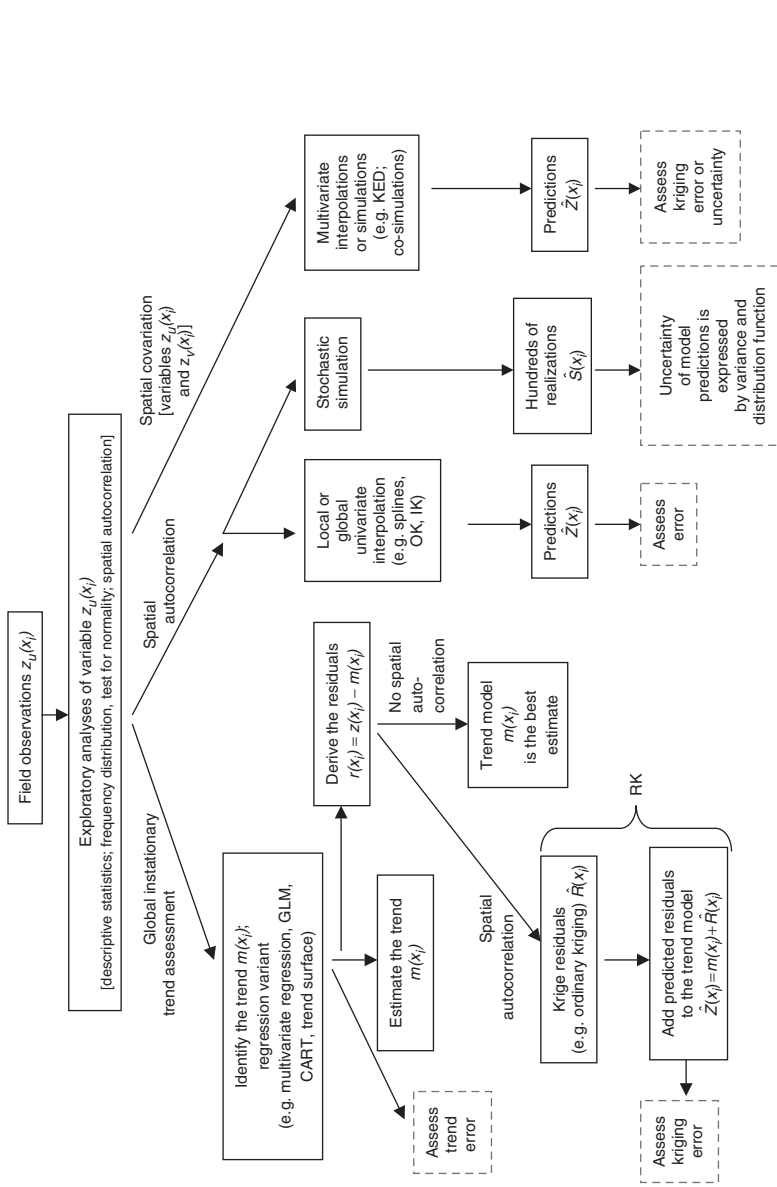
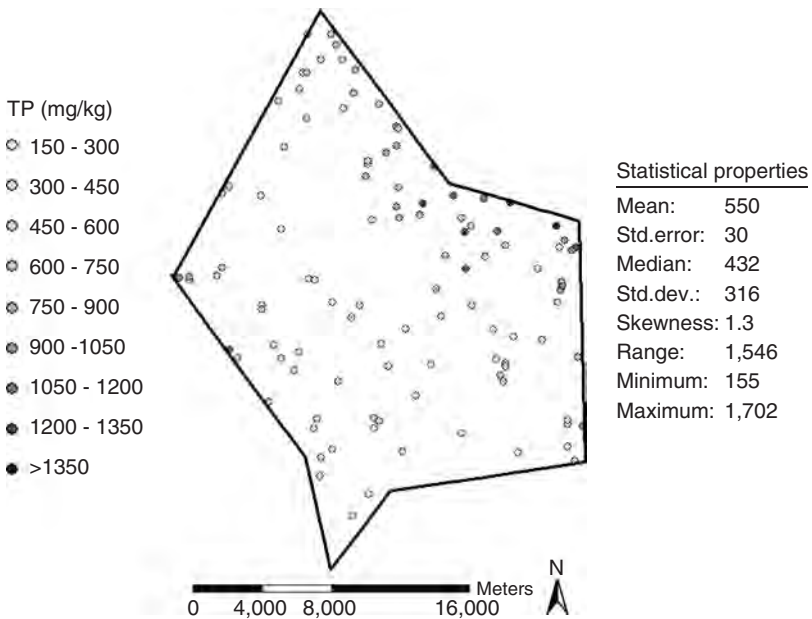


Figure 20.1. Decision flowchart for spatial modeling of biogeochemical soil properties.

1
3
5
7
9
11
13
15
17
19
21
23
25
27
29
31
33
35
37
39
41

1 has been strongly linked to productivity and community structure of
2 macrophytes (McCormick et al., 2002).

3 In 2003, we collected soil samples at 0–10 cm depth at 111 sites based
4 on a stratified random sampling design, spatially distributed throughout
5 WCA-2A that were analyzed for TP. Strata were derived using historic
6 ecological data layers such as the Normalized Difference Vegetation In-
7 dex as a proxy for vegetative communities, as well as soil and hydrologic
8 data. The sampling design was optimized to account for short-, medium-
9 and long-range variability of attributes. A map that shows the distribu-
10 tion of soil observations is shown in Fig. 20.2. Total P was measured with
11 a dry ashing procedure (Anderson, 1976) followed by determination with
12 an automated colorimetric procedure (U.S. Environmental Protection
13 Agency, 1993, Method 365.1). We complemented the soil dataset with an
14 exhaustive ancillary dataset derived from Advanced Spaceborne Thermal
15 Emission and Reflection Radiometer (ASTER) satellite image. The AS-
16 TER sensor covers a wide spectral range and high spatial and radiometric
17 resolutions. The spectral region is covered by three telescopes, three Vis-
18 ible and Near Infrared Radiometer (VNIR) bands with a spatial resolu-
19 tion of 15 m, six Short Wave Infrared Radiometer (SWIR) bands with a



41 *Figure 20.2.* Observations of total phosphorus (TP) at 0–10 cm depth measured at 111
locations across WCA-2A.

1 spatial resolution of 30 m and five thermal Infrared Radiometer (TIR)
bands with a spatial resolution of 90 m (Abrams et al., 2002). For the
3 purpose of this study, we used ASTER bands 2 and 3 (red and near-
infrared) from the VNIR spectral region in order to calculate the Nor-
5 malized Difference Vegetation Index (NDVI) (Rouse et al., 1974), which
is slightly different when compared to the NDVI derived from Landsat
7 satellite images that use bands 3 and 4.

Descriptive statistics of TP are enclosed in Fig. 20.2 and indicate a
9 positively skewed distribution with a skewness coefficient of 1.3, mean of
550, median of 432, minimum of 155 and maximum of 1702 mg kg⁻¹. To
11 predict TP across the WCA-2A we used completely regularized splines
with different neighborhood options (Fig. 20.3). The spline map in
13 Fig. 20.3c shows the smoothing effect of using a large local neighborhood
with 15 observations (minimum of 5) to predict TP at unsampled loca-
15 tions. In contrast, spline map 1 (Fig. 20.3a) shows blocky spatial patterns
due to the small local neighborhood with few (6) observations (minimum
17 of 2) that contributed to the predictions of TP at unsampled locations.
The mean prediction error for was lowest for spline map 2 with 0.4688,
19 followed by spline map 3 with -3.631 and spline map 1 with -4.598. The
RMSE was similar for spline map 3 with 252 and spline map 2 with 253
21 and highest for spline map 1 with 293. Here, a heuristic approach was
used to identify the interpolation method that showed the lowest predic-
23 tion errors.

To explore the spatial autocorrelation of TP, h-scattergrams and semi-
25 variograms were generated (Fig. 20.4). Just as the scattergram is a plot of
all pairs of values related to two different attributes measured at the same
27 location, the h-scattergram is a plot of all pairs of measurements ($z(x_i)$,
 $z(x_i + h)$) on the same attribute z at locations separated by a given dis-
29 tance h in a particular direction. A perfect correlation would entail that
all points in the h-scatter diagram lie on the line of equal values. As seen
31 in Fig. 20.4, the spread of the points indicated the variability of TP
values. The increasing inflation of the cloud in all h-scattergrams com-
33 puted in four different directions reflected the increasing dissimilarity
between observations farther apart. Overall, no distinct different patterns
35 in the directional h-scatter diagram were found indicating isotropic spa-
tial distributions. Isotropic means that the spatial patterns are the same/
37 similar in different directions.

Because the TP data were non-Gaussian we transformed TP values
39 with a log transformation to approximate a normal distribution. The
omnidirectional experimental semivariogram of log TP is shown in
41 Fig. 20.4b that was fitted with an exponential model with a nugget of
0.0185, sill 0.0512 and range of 7468 m. At the range the spatial

1
3
5
7
9
11
13
15
17
19
21
23
25
27
29
31
33
35
37
39
41

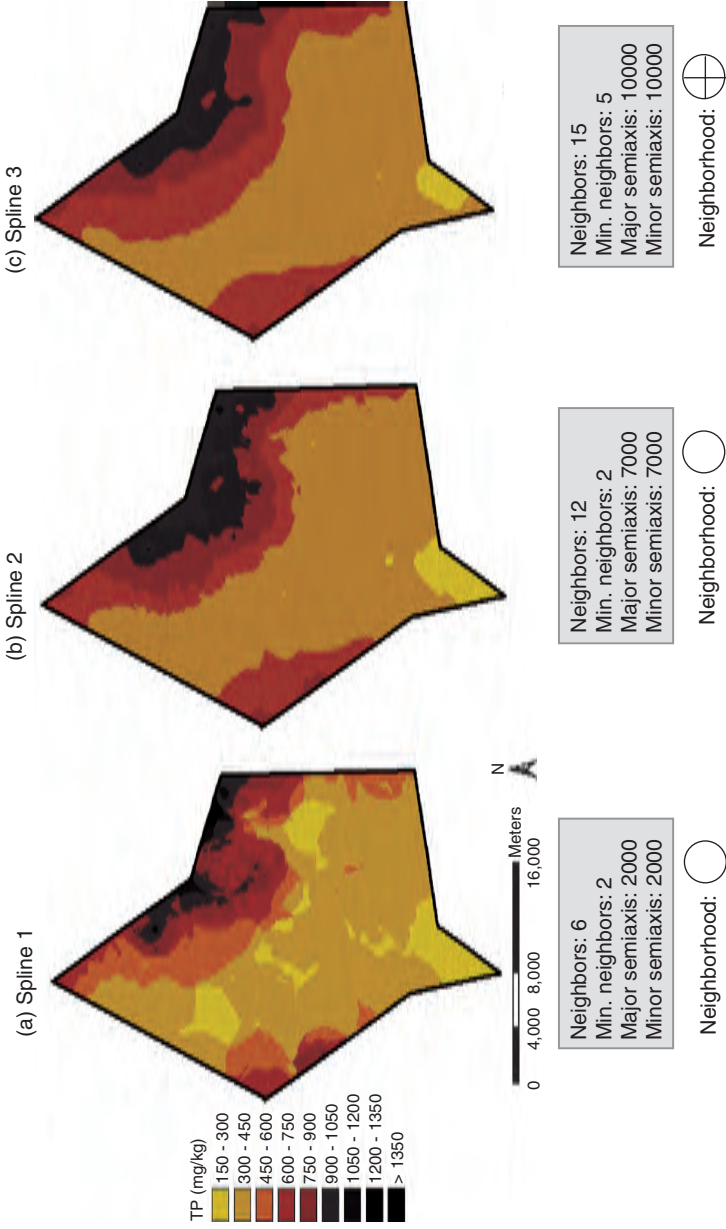


Figure 20.3. Predictions of TP derived from Completely Regularized Splines with different local neighborhood options.

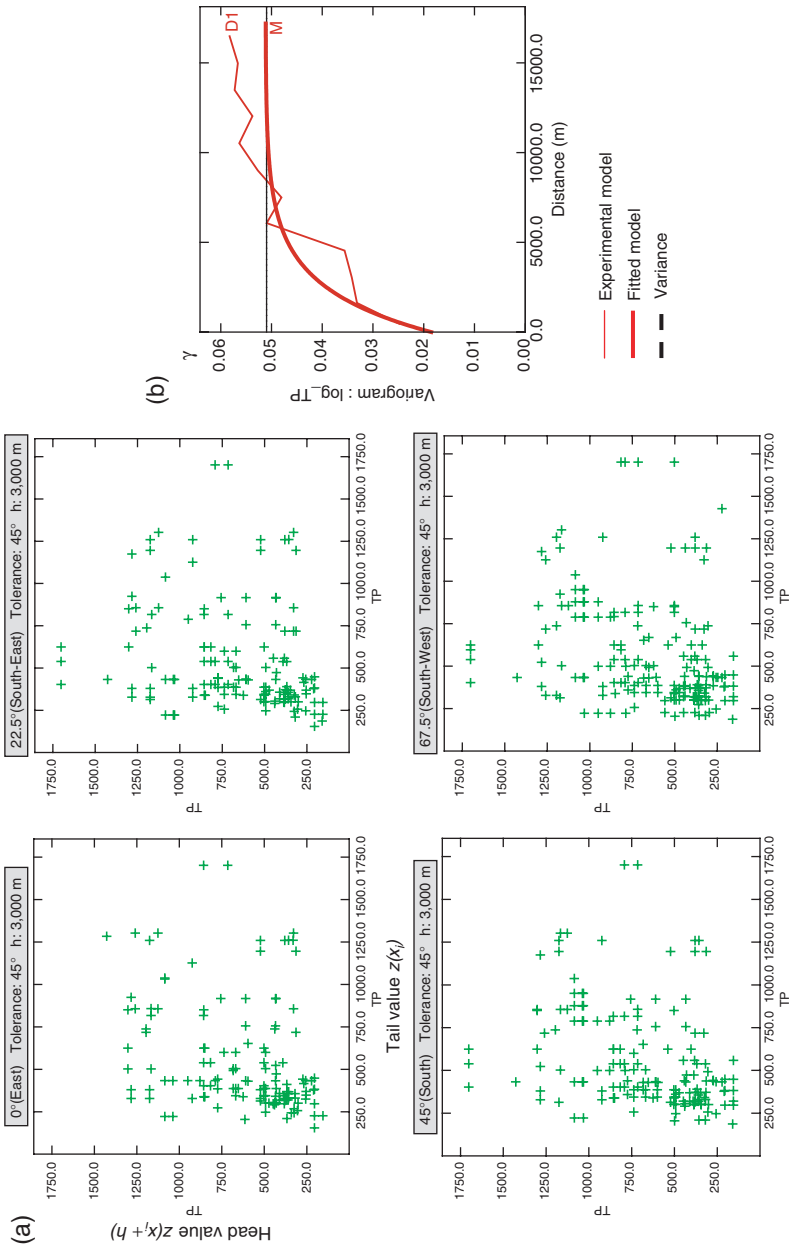


Figure 20.4. (a) h-scattergrams and (b) semivariogram of log TP.

1 autocorrelation becomes 0 indicating that this separation distance h
2 marks the limit of spatial dependence. Observations taken further apart than the range
3 are spatially independent. Experimental semivariograms were computed using Eq. (3) in four directions (0, 45, 90 and 135°) to
4 reveal anisotropy in the variation. Anisotropy describes directional spatial structures. Due to the limited amount of data pairs available for
5 different directions it was difficult to identify any clear directional trends. Although there is a hydraulic gradient in WCA-2A that extends from the
6 northeastern canal into the west-south direction we could not confirm these trends in the soil TP dataset. Therefore, we proceeded with the
7 omnidirectional fitted semivariogram model. We used a search neighborhood of 7468 m; 1 angular sector; a minimum number of observations
8 of 4 and an optimum number of observations of 10 to predict TP at unsampled locations using OK. The OK prediction map is shown in
9 Fig. 20.5. Based on cross-validation the mean prediction error was -41.77 indicating a slight underestimation of true observations and a
10 root mean square prediction error of 257 mg kg^{-1} . The coefficient of

19
21
23
25
27
29
31
33
35
37
39
41

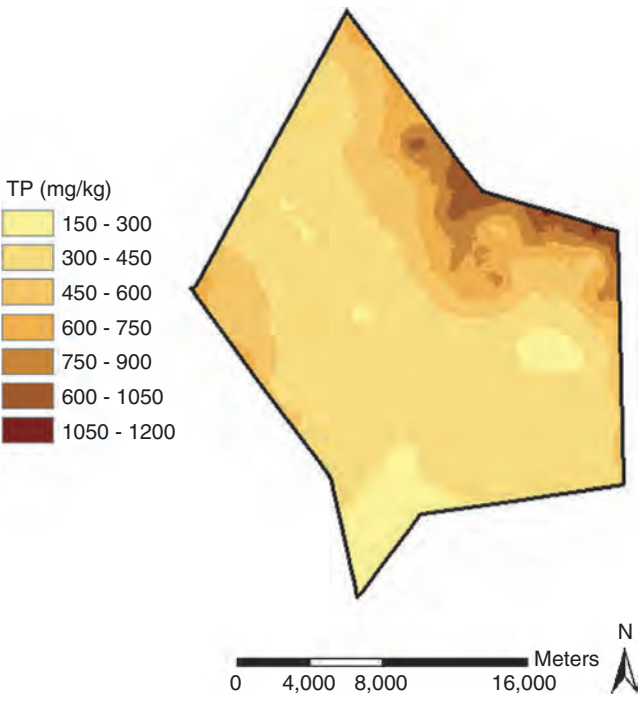


Figure 20.5. Predictions of TP based on Ordinary Kriging.

1 determination (R^2) between measured TP and estimated TP was 0.82
2 indicating good predictions. To highlight differences between TP predic-
3 tions derived from our spatially distributed observations and observa-
4 tions along a linear corridor (transect) we created a subset of observations
5 extending along a previously identified TP gradient (Reddy et al., 1997;
6 DeBusk et al., 2001). The corridor extended from the hydrologic bound-
7 ary in the east into the interior of the marsh to the south-west boundary
8 (Fig. 20.6a). Total phosphorus observations were predicted based on 10
9 observations along the linear corridor using OK. We derived a difference
10 map by subtracting the TP predictions made along the linear corridor
11 from the TP predictions derived from the spatially distributed design
12 (Fig. 20.6b). The difference map shows deviations of more than -240 up
13 to 180 mg kg^{-1} TP illustrating the large differences between both predic-
14 tion maps. This example illustrates the limitations of sparse biogeochem-
15 ical datasets based on only 10 observations along a corridor. Sparse
16 datasets along corridors/transects have major limitations to map the un-
17 derlying spatial variability. In the eastern part of WCA-2A, low TP values
18 (328 and 380 mg kg^{-1}) coexisted with very high TP values (1259 mg kg^{-1})
19 in close proximity (Fig. 20.6b). In contrast, over large distances from the
20 interior of the marsh to the south-west hydrologic boundary, TP values
21 were relatively invariant at different lags ranging from 257 to 371 mg kg^{-1}
22 TP.

23 Prediction maps are valuable to characterize the spatial distribution
24 and variability of biogeochemical properties such as TP. However, to
25 assess the impact of biogeochemical properties exceeding thresholds that
26 stimulate net productivity and turnover rates is important to characterize
27 the ecological integrity and structure of an ecosystem. Thus, we used IK
28 to derive the probabilities of TP being above a respective cutoff value (z_k)
29 of 450 , 500 , 550 , 600 , 650 and 700 mg kg^{-1} (Fig. 20.7). For reference
30 purposes, historical background TP concentrations in WCA-2A have
31 been estimated to be 500 mg kg^{-1} (DeBusk et al., 2001). Probability maps
32 are well suited for decision makers demonstrating the outcome ranging
33 from conservative assumptions (low threshold value) to liberal assump-
34 tions (high threshold value). Hot spots can be well identified using IK
35 highlighting the extreme values that exceed the background concentra-
36 tions.

37 Stochastic simulations emphasize the uncertainty associated with predic-
38 tions of biogeochemical properties generating hundreds or thousands
39 of realizations. We used CSGS to generate 100 realizations of TP
40 (Fig. 20.8) using the following modeling options: dilation radius of 20 in
41 the x and y direction; 15 maximum number of data nodes; and 5 max-
imum number of simulation nodes. The E-type map of the mean showed

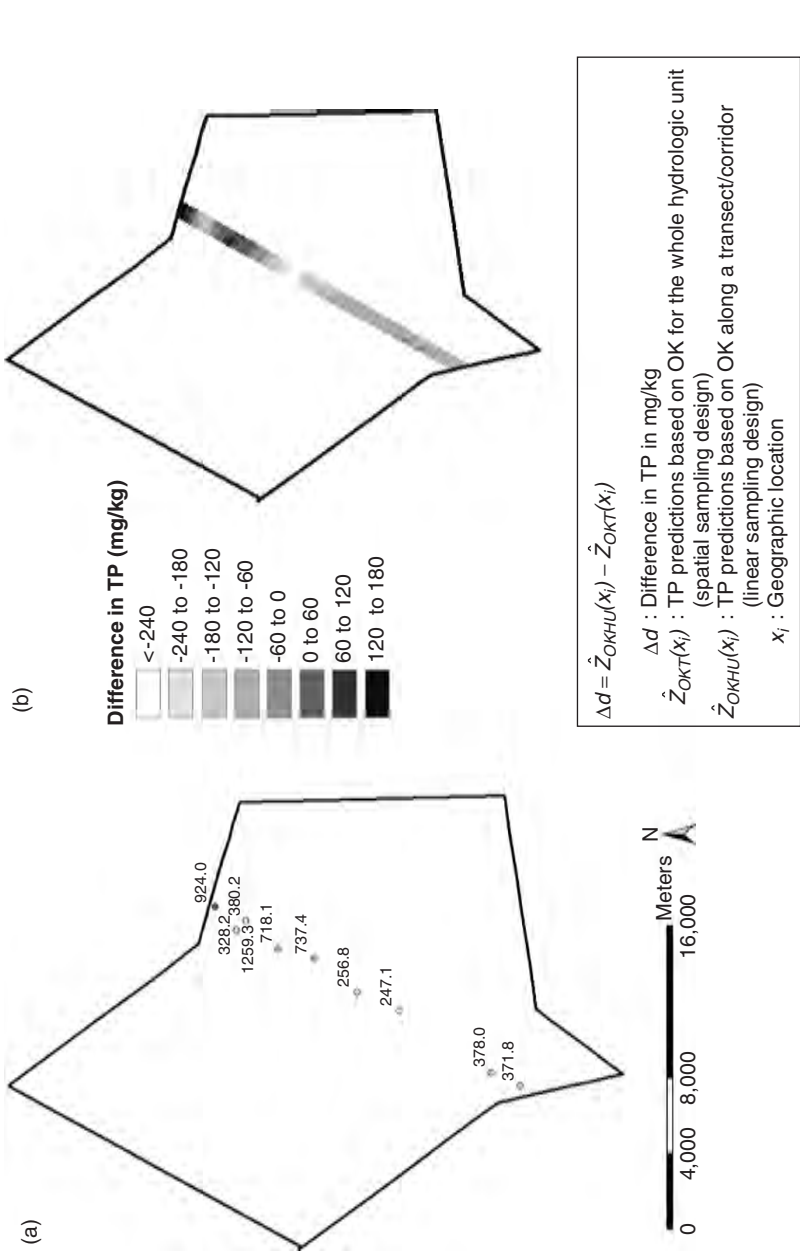


Figure 20.6. (a) Transect/corridor along TP gradient extending from the hydrologic boundary into the marsh interior. Map shows point TP observations in mg kg^{-1} . (b) Map shows the difference in TP predictions along the transect/corridor derived from a spatial and linear sampling design.

1
3
5
7
9
11
13
15
17
19
21
23
25
27
29
31
33
35
37
39
41

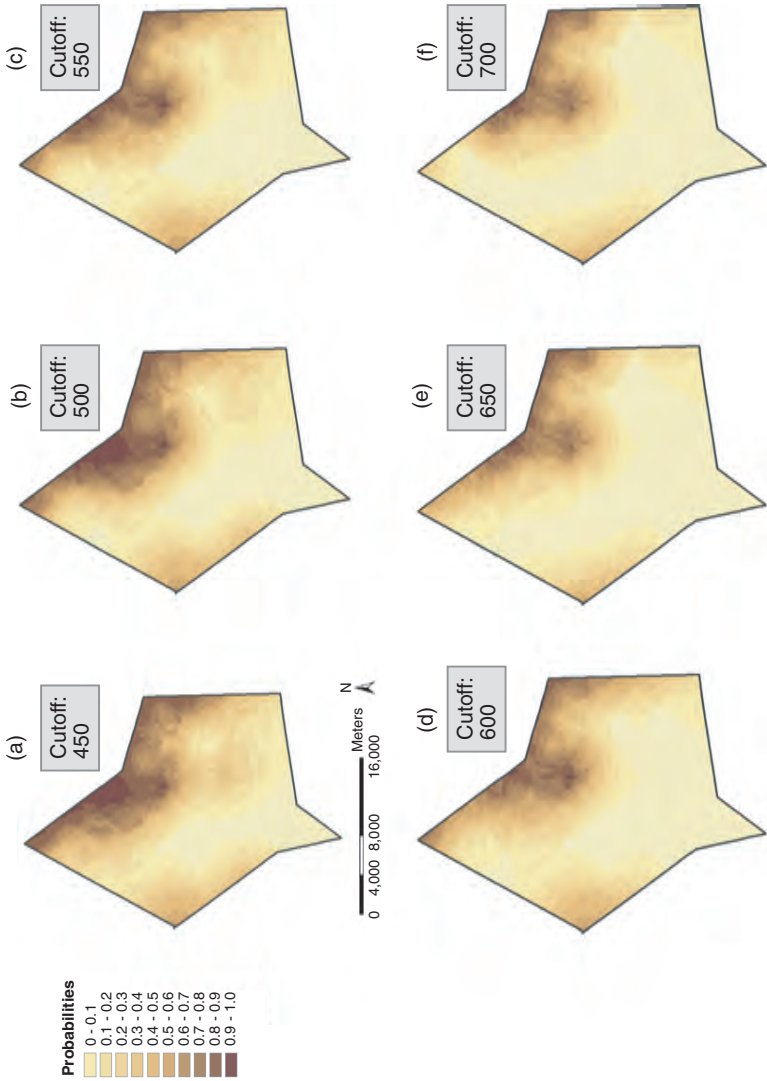


Figure 20.7. Probabilities of being above respective TP cutoff values derived from Indicator Kriging.

1
3
5
7
9
11
13
15
17
19
21
23
25
27
29
31
33
35
37
39
41

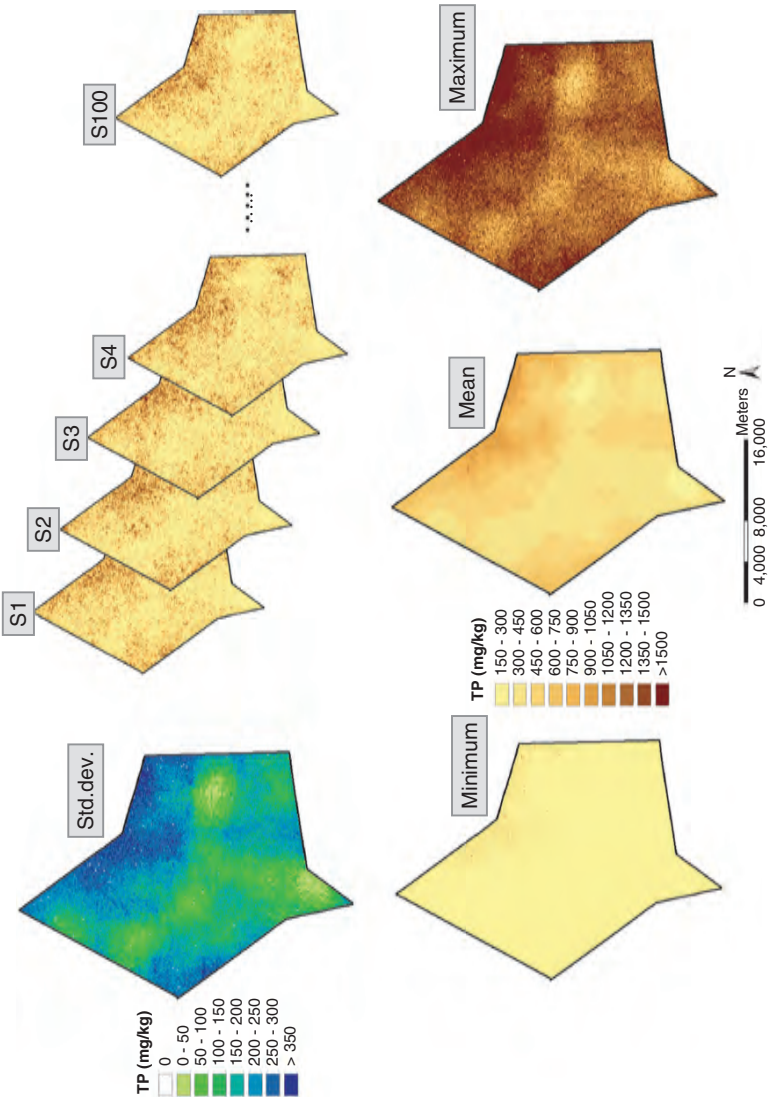


Figure 20.8. Minimum, mean, maximum and select realizations (S1, S2, S3, S4, S5, ..., S100) of TP generated with Conditional Sequential Gaussian Simulation. The uncertainty of predictions is expressed by the standard deviation (std. dev.)

1 similar patterns of TP as seen on the OK prediction map. However, the
2 TP patterns in Fig. 20.8 were much more speckled when compared to the
3 smooth OK prediction map. The uncertainty of TP predictions based on
4 CSGS was expressed using minimum and maximum realization maps that
5 show the range of realizations and the standard deviation map. The
6 largest uncertainty was found in the eastern part of WCA-2A coinciding
7 with high TP predictions. The lowest uncertainty was found in the in-
8 terior of the marsh extending south and eastwards mirroring the lowest
9 observed and predicted TP.

10 To improve predictions of TP we analyzed the relationships between
11 soil TP, spectral bands and the NDVI. The Spearman Correlation Co-
12 efficient (r) between TP and NDVI was high with 0.65. We used a step-
13 wise multiple regression to quantify the relationship between soil and
14 spectral data and derived the following algorithm:

$$15 \quad TP = 401.78 + 1890.77 * NDVI \quad \text{with an } R^2 \text{ of } 0.37 \text{ (} p = 0.001 \text{)}$$

16 This linear relationship was used as trend model to predict TP across
17 WCA-2A using the exhaustive NDVI pixel dataset. We derived residuals
18 by subtracting the trend model from the observations. The spatially au-
19 tocorrelated residuals were then kriged and residual predictions added to
20 the global trend model to generate the TP prediction map shown in
21 Fig. 20.9. The RK procedure showed an R^2 of 0.93, which was higher
22 than the one derived for OK (R^2 of 0.82). Overall, the TP prediction map
23 derived from RK showed similar patterns as seen on the OK prediction
24 map (Fig. 20.5) and the CSGS realization maps (Fig. 20.8). However,
25 predictions in Fig. 20.9 highlighted landscape features such as vegetative
26 patterns, slough/ridge systems, open water, tree islands, etc. mapped
27 through the NDVI index that showed quantitative linkages to soil TP.
28 Predictions derived from RK do not honor observed data values and have
29 limitations to describe the uncertainty of predictions. This is the strength
30 of stochastic simulations that are focused to characterize the uncertainty
31 of predictions.

32 In Fig. 20.10 we contrast the different geospatial methods and TP
33 observations in terms of their distribution functions. Predictions based on
34 RK and realizations derived from CSGS showed the closest match to the
35 distribution of TP observations. In particular, the high TP values above
36 1050 mg kg⁻¹ were well represented in the RK and CSGS maps.

37

38

39

40

41

1
3
5
7
9
11
13
15
17
19
21
23
25
27
29
31
33
35
37
39
41

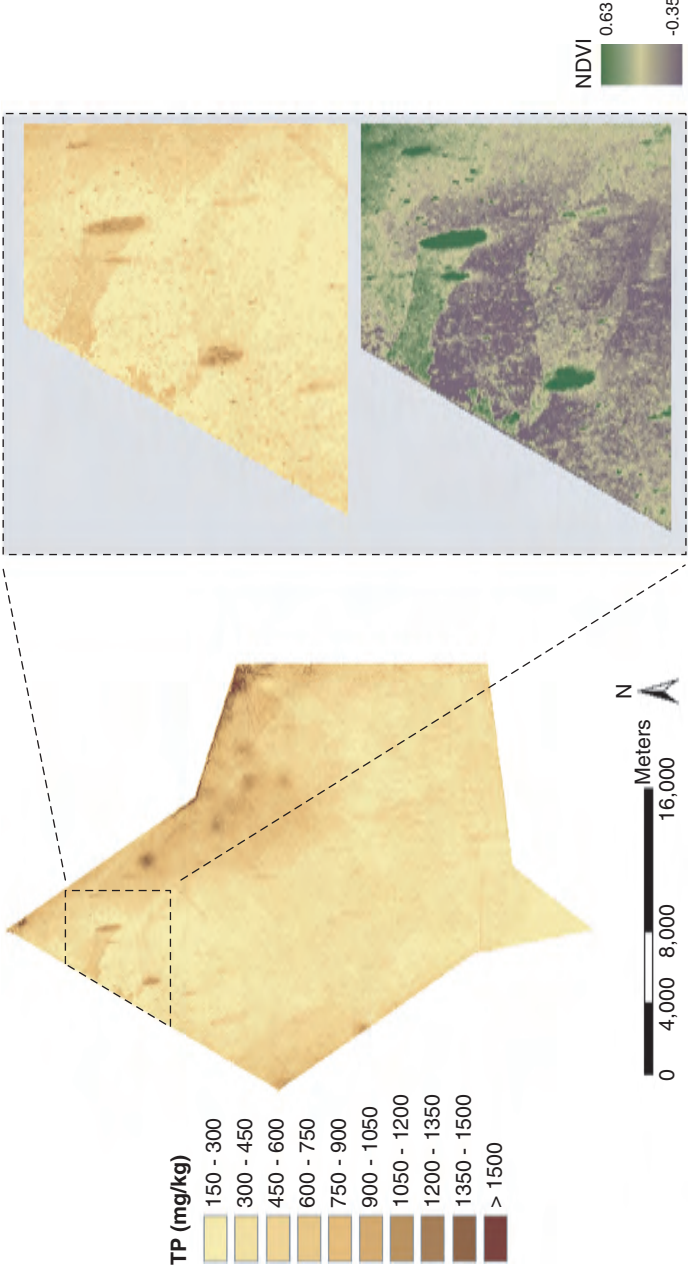


Figure 20.9. Left: Predictions of TP derived from Regression Kriging. Right: Close-up of TP predictions and NDVI map depicting landscape features such as tree islands and vegetation structures.

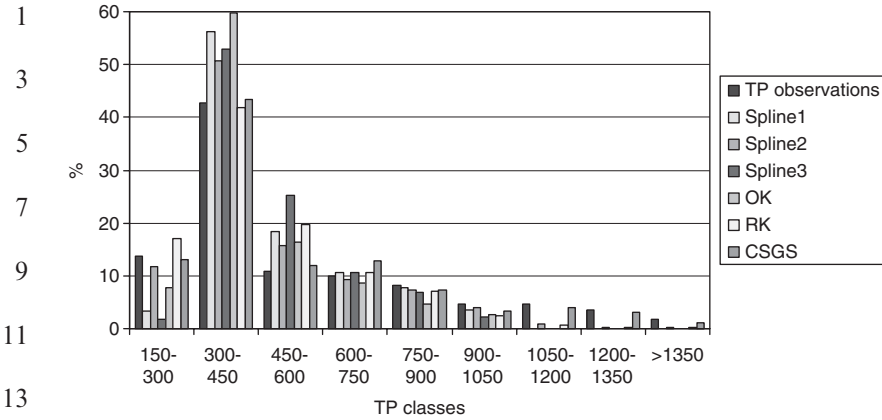


Figure 20.10. Distribution functions of TP observations, predictions and realizations generated with different interpolation methods.

20.4. Remarks

Considering the complexity of wetland ecosystems it is essential to employ spatially distributed sampling designs and geospatial prediction methods that have the ability to characterize the underlying spatial distribution and variability of biogeochemical properties. The integration of sparse point observations of biogeochemical properties and dense ancillary environmental datasets has the potential to improve spatially explicit predictions of properties throughout aquatic (and terrestrial) ecosystems. For example, remote sensing data are cost-effective and provide exhaustive, high-resolution information at landscape-scale. In this chapter we focused on spatially explicit mapping of soil biogeochemical properties exemplified by TP. The case study demonstrated that OK, IK, RK and CSGS produced different maps using the same TP observations. All maps are valid in the sense that they describe the spatial patterns of TP in this specific wetland. Since different geostatistical methods aim at different goals (e.g., to minimize the variance, assess the uncertainty of model predictions, etc.) we have to use them cautiously. Multi-variate geostatistical and hybrid methods that incorporate ancillary environmental data to model biogeochemical properties have much potential to improve our understanding of aquatic and terrestrial ecosystems. To document the evolution of biogeochemical properties through time more monitoring programs are in need. Bridging the gaps between micro, meso and macro spatial scales will be the challenge of future research in aquatic and terrestrial biogeochemistry.

1 **ACKNOWLEDGEMENTS**

3 Funding was provided by the South Florida Water Management District
 4 and varied other federal sources. We would like to thank Todd Z. Os-
 5 borne (Soil and Water Science Dept, UF), Sue Newman (South Florida
 6 Water Management District) and Terry Jones (Aircoastal Helicopter) to
 7 assist with data collection; Yu Wang of the Wetland Biogeochemistry
 8 Laboratory for her assistance with the laboratory analyses. This research
 9 was supported by the Florida Agricultural Experiment Station and ap-
 10 proved for publication as Journal Series No. R-10817.

11

13 **REFERENCES**

- 15 Abrams, M., Hook, S., Ramachandran, B., 2002. ASTER user handbook. Version 2. Pas-
 16 adena, CA; Jet Propulsion Laboratory, Sioux Fall, SD, EROS Data Center.
- 17 Anderson, J.M., 1976. An ignition method for determination of total phosphorus in lake
 18 sediments. *Water Res.* 10, 329–331.
- 19 Berthouex, P.M., Brown, L.C., 2002. *Statistics for Environmental Engineers*. Lewis, New
 20 York, p. 489.
- 21 Burrough, P.A., 1986. *Principles of geographical information systems for land resources*
 22 *assessment*. Clarendon Press, UK, p.194.
- 23 Burrough, P.A., McDonnell, R.A., 1998. *Principles of geographical information systems—*
 24 *spatial information systems and geostatistics*. Oxford University Press, Oxford, UK,
 25 p. 333.
- 26 Bruland, G.L., Richardson, C.J., 2005. Spatial variability of soil properties in created, re-
 27 stored and paired natural wetlands. *Soil Sci. Soc. Am. J.* 69, 273–284.
- 28 Chilès, J.-P., Allard, D., 2005. Stochastic simulation of soil variations. In: Grunwald, S.
 29 (Ed.), *Environmental Soil-Landscape Modeling—Geographic Information Technol-*
 30 *ogies and Pedometrics*. CRC Press, New York, pp. 289–323.
- 31 Chilès, J.-P., Delfiner, P., 1999. *Geostatistics—Modeling Spatial Uncertainty*. Wiley-Inter-
 32 science, New York, p. 695.
- 33 Craft, C.B., Chiang, C., 2002. Forms and amounts of soil nitrogen and phosphorus across a
 34 longleaf pine-depressional wetland landscape. *Soil Sci. Soc. Am. J.* 66(5), 1713–1721.
- 35 DeBusk, W.F., Newman, S., Reddy, K.R., 2001. Spatial and temporal patterns of soil
 36 phosphorus in Everglades Water Conservation Area 2A. *J. Environ. Qual.* 30, 1438–
 37 1446.
- 38 Fisher, R.A., 1925. *Statistical methods for research workers*. Oliver and Boyd, Edingurgh,
 39 Scotland, p. 189.
- 40 Fisher, M.M., Reddy, K.R., 2001. Phosphorus flux from wetland soils affected by long-term
 41 nutrient loading. *J. Environ. Qual.* 30(1), 261–271.
- Geary, R.C., 1954. The contiguity ratio and statistical mapping. *Incorporated Statistician* 5,
 115–145.
- Goovaerts, P., 1997. *Geostatistics for natural resources evaluation*. Oxford University Press,
 New York, p. 483.
- Goovaerts, P., 1999. Geostatistics in soil science: State-of-the-art and perspectives. *Geode-*
 rma 89, 1–45.

- 1 Grunwald, S., 2005. What do we really know about the space-time continuum of soil-
landscapes?. In: Grunwald, S. (Ed.), *Environmental Soil-Landscape Modeling—Ge-*
3 *ographic Information Technologies and Pedometrics*. CRC Press, New York, pp. 3–
37.
- 5 Grunwald, S., Corstanje, R., Weinrich, B.E., Reddy, K.R., in press. Spatial pattern of labile
forms of phosphorus in a subtropical wetland. *J. Environ. Qual.* 000, 00–00.
- 7 Grunwald, S., Reddy, K.R., Newman, S., DeBusk, W.F., 2004. Spatial variability, distri-
bution and uncertainty assessment of soil phosphorus in a south Florida wetland.
Environmetrics 15, 811–825.
- 9 Hengl, T., Heuvelink, G.B.M., Stein, A., 2004. A generic framework for spatial prediction of
soil variables based on regression-kriging. *Geoderma* 120, 75–93.
- 11 Holling, C.S., Gunderson, L.H., 2002. Resilience and adaptive cycles. In: Gunderson, L.H.,
Holling, C.S. (Eds.), *Panarchy: Understanding Transformations in Human and Natu-*
ral Systems. Island Press, Washington, D.C., p. 287.
- 13 Isaaks, E.H., Srivastava, R.M., 1989. *An introduction to applied geostatistics*. Oxford Uni-
versity Press, New York, p. 289.
- 15 Karathanasis, A.D., Thompson, Y.L., Barton, C.D., 2003. Long-term evaluations of sea-
sonally saturated wetlands in western Kentucky. *Soils Sci. Soc. Am. J.* 67(2), 662–
673.
- 17 Levin, S.A., 1992. The problem of pattern and scale in ecology. *Ecology* 73, 1943–1967.
- 19 McBratney, A.B., Odeh, I.O.A., Bishop, T.F.A., Dunbar, M.S., Shatar, T.M., 2000. An
overview of pedometric techniques for use in soil survey. *Geoderma* 97, 293–327.
- 21 McBratney, A.B., Mendonça Santos, M.L., Minasny, B., 2003. On digital soil mapping.
Geoderma 117, 3–52.
- 23 McCollum, S.H., Carlisle, V.W., Volk, B.G., 1976. Historical and current classification of
organic soils in the Florida Everglades. *Proc. Soil Crop Sci. Soc. FL* 35, 173–177.
- 25 McCormick, P.V., Newman, S., Miao, S., Gawlik, D., Marley, D., Reddy, K.R., Fontaine,
T., 2002. Effects of anthropogenic phosphorus inputs on the Everglades. In: Porter,
J.W., Porter, K.G. (Eds.), *The Everglades, Florida Bay, and Coral Reefs of the*
Florida Keys: An Ecosystem Sourcebook. CRC Press, Boca Raton p. 1000.
- 27 Mitsch, W.J., Gosselink, J.G., 2000. *Wetlands*. Wiley, New York, p. 920.
- 29 Moran, P.A.P., 1950. Notes on continuous stochastic phenomena. *Biometrika* 37, 17–23.
- 31 Morris, D.R., Glaz, B., Daroub, S.H., 2004. Organic matter oxidation potential determi-
nation in a periodically flooded Histosol under sugarcane. *Soil Sci. Soc. Am. J.* 68,
994–1001.
- 33 Newman, S., Reddy, K.R., DeBusk, W.D., Wang, Y., Shih, G., Fisher, M.M., 1997. Spatial
distribution of soil nutrients in a northern Everglades marsh: Water Conservation
Area 1. *Soil Sci. Soc. Am. J.* 61, 1275–1283.
- 35 Noe, G.B., Childers, D.L., Jones, R.D., 2001. Phosphorus biogeochemistry and the impact
of phosphorus enrichment: Why is the Everglades so unique. *Ecosystems* 4, 603–624.
- 37 Odeh, I.O.A., McBratney, A.B., 2000. Using AVHRR imageries for spatial prediction of
clay content in the lower Namoi Valley of Eastern Australia. *Geoderma* 97, 237–254.
- 39 Odeh, I.O.A., McBratney, A.B., Chittleborough, D.J., 1994. Spatial prediction of soil
properties from landform attributes derived from a digital elevation model. *Geode-*
rma 63, 197–214.
- 41 Odeh, I.O.A., McBratney, A.B., Chittleborough, D.J., 1995. Further results on prediction of
soil properties from terrain attributes: Heterotopic cokriging and regression-kriging.
Geoderma 67, 215–226.
- Porter, J.W. and K.G. Porter, (Eds.), 2002, *The Everglades, Florida Bay and Coral Reefs of
the Florida Keys—An Ecosystem Sourcebook*. CRC Press, New York p. 1000.

- 1 Reddy, K.R., Wang, Y., DeBusk, W.F., Fisher, M.M., Newman, S., 1998. Forms of soil
phosphorus in selected hydrologic units of Florida Everglades ecosystems. *Soil Sci.*
3 *Soc. Am. J.* 62(4), 1134–1147.
- 5 Reddy, K.R., White, J.R., Wright, A., Chua, T., 1997. Influence of phosphorus loading on
microbial processes in the soil and water column of wetlands. In: Reddy, K.R.,
O'Connor, G.A., Schelske, C.L. (Eds.), *Phosphorus Biogeochemistry in Subtropical*
7 *Ecosystems*. Lewis, New York, p. 707.
- 9 Rouse, J.W., Haas, R.H., Schell, J.A., Deering, D.W., 1974. Monitoring vegetation systems
in the Great Plains with ERTS. *Proceedings, third Earth Resources Technology*
11 *Satellite-1 Symposium, Greenbelt: NASA SP-351*, pp. 3010–3017.
- 13 Turner, M.G., O'Neill, R.V., Gardner, R.H., Milne, B.T., 1989. Effects of changing spatial
scale on the analysis of landscape pattern. *Landscape Ecol.* 3(3/4), 153–162.
- 15 U.S. Environmental Protection Agency, 1993. *Methods for determination of inorganic*
substances in environmental samples. Environmental Monitoring Systems Lab,
17 Cincinnati, OH, USA.
- 19 Webster, R., 1994. The development of pedometrics. *Geoderma* 62, 1–15.
- 21 Webster, R., Oliver, M.A., 2001. *Geostatistics for environmental scientists*. Wiley, New
23 York, p. 271.
- 25 Webster, R., Oliver, M.A., 2005. Modeling spatial variation of soil as random functions. In:
27 Grunwald, S. (Ed.), *Environmental Soil-Landscape Modeling Geographic Information*
31 *Technologies and Pedometrics*. CRC Press, New York, pp. 241–289.
- 33 White, J.R., Reddy, K.R., 2000. Influence of phosphorus loading on organic nitrogen min-
35 eralization of Everglades soils. *Soil Sci. Soc. Am. J.* 64(4), 1525–1534.
- 37
- 39
- 41